Composites Part B: Engineering, Volume 60, April 2014, pp. 119-124
DOI: 10.1016/j.compositesb.2013.12.055

Buckling and post-buckling of a composite C-section with cutout and flange reinforcement

Shijun Guo[2], Daochun Li[1*], Xiang Zhang[2], Jinwu Xiang[1]

[1]School of Aeronautics Science and Technology, Beihang University, Beijing, 100191 PR China

[2]Aerospace Engineering, School of Engineering, Cranfield University, Cranfield, Bedford, MK43 0AL, UK

Abstract. This paper presents an investigation into the effect of cutout and flange reinforcement on the buckling and post-buckling behaviour of a carbon/epoxy composite C-section structure. The C-section having a cutout in the web is clamped at one end and subjected to a shear load at the other free end. Three different stiffener reinforcements were investigated in finite element analysis by using MSC Nastran. Buckling load was predicted by using both linear and nonlinear FE analysis. Experiments were carried out to validate the numerical model and results. Subsequently post-buckling analysis was carried out by predicting the load-deflection response of the C-section beam in nonlinear analysis. Tsai-Wu failure criterion was used to detect the first-play-failure load. The effect of circular and diamond cutout shape and effective flange reinforcements were investigated. The results show that the cutout and reinforcement have little effect on the buckling stability. However an L-shape stiffener to reinforce the C-section flange can improve the critical failure load by 20.9%.

Keywords: Carbon-fibre composites; discontinuous reinforcement; buckling; post-buckling

Nomenclature

E_i	=	ply modulus in the *i*-direction
G_{ij}	=	ply shear modulus in the *i-j* plane
ν_{12}	=	ply Poisson's ratio in the 1-2 plane
X_t, X_C	=	tensile/compressive strength in fibre direction
Y_t, Yc	=	tensile/compressive strength in transverse direction
S	=	shear strength
ρ	=	density of the composite
σ_1	=	maximum principal stress

1. Introduction

Carbon reinforced composite materials are being increasingly used in primary airframes due to many advantages over the traditional metallic alloys. Research efforts have been made to further improve the structural design and mechanical performance in application. In this paper attention was focused on the buckling and post-buckling behaviour and design improvement of a composite C-section beam. This configuration may represent part of a typical wing or tail-plane spar structure. Since cutouts on the web are part of the structure features for weight saving or system access, their effect on the structural load carrying capability is one of the primary concerns in airframe design. Another concern is the buckling stability of the C-section especially the flange that is subjected to compressive force. The influence and

* Corresponding author. Tel.: +8610 82338786; fax: +8610 82317755
E-mail address: lidc@buaa.edu.cn (D. Li)

reinforcement of the cutout on the C-section web on the flange buckling and failure should be quantified for this type of thin-walled structures.

Extensive research has been carried out for stress analysis around flat composite panels by analytical or numerical methods [1-4]. Studies were also performed in finding optimised cutout shape, e.g. Falzon et al [5] showed that for a quasi-isotropic panel under in-plane shear load the optimum cutout shape was a diamond rather than the conventional circular. From the results of Kumar and Singh [6], quasi-isotropic laminate under combined in-plane loads with elliptical vertical cutout has the maximum buckling load and post-buckling strengths, whereas the laminate with elliptical-horizontal cutout has the minimum strengths. With the same composite laminate and loads, the effects of flexural boundary conditions on buckling and post-buckling responses with and without a central cutout of various shapes was carried out using finite element method [7]. Various cutout edge reinforcements were investigated to reduce stress concentration and increase buckling strength [8]. This result was further investigated for the C-section beam in a previous study [9] and relevant to this current research.

Cutout location and size also influence a composite panel's buckling stability. A comprehensive review on bucking and post-buckling behaviour of composite plates was published by Nemeth [10]. The review includes many influential factors, such as the cutout size, shape, eccentricity and orientation, plate aspect and slenderness ratios, loading and boundary conditions, and plate orthotropy and anisotropy. A further study on the post-buckling behaviour was conducted by Bailey and Wood [11], in which the influence of cutout diameter to panel length ratio (up to 0.65) on the load carrying capability was investigated. The study has shown that a ratio greater than 0.35 will result in higher buckling load that is even greater than that of a panel without a cutout. This is due to the change in load paths and stress redistribution. In a panel without a cutout a great portion of the pre-buckling axial load is centrally located; therefore the bending stiffness of the central part of the panel is of paramount importance. Research has shown that bending stiffness and buckling resistance are reduced when relatively small cutouts are introduced. However, when a relatively larger cutout is present, the load path is no longer centrally located but directed towards the edges of the panel. This explains why the buckling stability is greater for panels with larger cutouts. In this regard, Eiblmeier and Loughlan studied the buckling response of a composite laminate panel with reinforced circular cutout under different loading and boundary conditions [12-13].

Lateral buckling is one of the most important mechanical behaviour of composite beams subjected to certain external loads. The effects of hole diameter and hole location on the lateral buckling behaviour of woven fabric laminated composite cantilever beams were investigated by Eryigit et al [14]. Pasinli [15] studied the similar cantilever beams but having two square or two circular holes by using theoretical, experimental and numerical methods. It was concluded that the circular holes are advantageous compared to the square ones in terms of lateral buckling behaviour. Cylindrical shell is one of the important structures used widely in engineering applications. Buckling and post-buckling of these shells is a necessary fundamental problem and has been attracted attention of many researchers [16]. Shi et al [17] investigate the local and global buckling responses of composite grid stiffened cylindrical shells with unreinforced or reinforced cutouts under axial compressive loading. The results indicated that the grid reinforcements can reduce or eliminate the risk of local buckling response near the cutout areas and increase the critical load more effectively than the skin reinforcements.

Research on the fibre tow placement (or fibre tow steering) technique has been conducted recently in order to reduce cutout stress concentrations. Jegley et al. [18] demonstrated the effectiveness of fibre tow steered panels in reducing the stress concentration and improving the overall panel load carrying capability under both compressive and shear loads. Lopes et al [19] carried out a study on the post-buckling progressive damage behaviour and final structural failure of tow-placed composite panels with a central cutout. Panels with fibre tow reinforced cutout showed up to 56% higher strength compared with the straight fibre laminates. Initiation of damage and final structural failure were also delayed significantly for the fibre tow reinforced panels.

Apart from the aforementioned studies on flat plates, buckling behaviour of composite C-section beams has also been reported in the open literature. For example, Razzaq et al [20] focused on the effect of load position and warping on the buckling of a simply supported C-section beam under two point loads applied symmetrically about the beam's mid-span. It was found that the warping effect was most severe when the load was applied thought the centroid; stresses due to warping were over 20% higher than the flexural stresses. Lee and Kim [21] developed a finite element model to study the lateral buckling of a composite C-section beam. The effects of fibre orientation, location and type of applied load on critical buckling load were studied. The results showed that, for a simply supported beam, the warping effect was reduced by rotating the fibre angle off-axis up to 45°. This material layup has increased the critical buckling load of relatively long beams, but decreased the buckling stability of short beams (in which the optimal fibre direction was 0°). Shan and Qiao [22] derived a total potential energy method for a composite cantilever beam and conducted an analytical study of buckling due to bending and torsion considering various parameters such as the load location, fibre orientation and fibre volume fraction.

However, few studies have been published to address the cutout influence on the buckling and post-buckling behaviour of C-section composite beams. This current paper presents a study on cutout effect and flange reinforcement to improve bucking and post-buckling stability of a C-section beam. An experiment was conducted to validate the finite element model and analysis. Different cutout and reinforcement effects on the C-section buckling and post-buckling behaviour were studied and flange reinforcement was presented to improve the structure stability and strength.

2. Model and Methodology

2.1. Material and geometry

Three constant C-section beams with and without a web cutout were studied. The beam is 650 mm in length, 200 mm in web depth and 100 mm in flange width, as shown in Fig. 1a. It is made of 16 plies of the M21/T800S carbon-epoxy prepreg in a symmetric layup $[\pm45/0/\pm45/90/\pm45]_s$ for both the web and flanges. The ply thickness is 0.25 mm resulting in 4 mm thick laminate. Mechanical properties of the laminate are given in Table 1. One of the C-section has a circular cutout on the web and another with a diamond shape cutout. Three different cutout reinforcements were considered. Detailed geometry and dimension of the cutouts and reinforcements are shown in Fig. 1b. The steel reinforcement rings of 1.5 mm thick and 20 mm wide were made of T300 series stainless steel. The laminate rings were 2 mm thick and 20 mm wide cut from an eight-ply laminate made of the same material as the beam with stacking sequence $[0/\pm45/90]_s$. The fibre tow rings were made of six plies of 0.25 mm thick fibre tape.

In order to improve the buckling and post-buckling performance of the C-section beam, three flange reinforcements of L-shape stiffeners (Re1 – Re3) as shown in Fig. 2 were designed. They are made of the same material and layup as the beam and have the same weight. However the cross section, length and bonding position are different. The cross section of stiffener Re1 is twice of Re2, but half the length. The vertical stiffener Re3 has the same geometry size as Re1, but different bonding direction from the horizontal stiffeners Re1 and Re2. For each reinforcement design, only one of these stiffeners was used.

2.2. Numerical model and analysis

The C-section beam was numerically modelled and analysed by using the commercial package MSC Patran/Nastran. The beam and reinforcement rings were modelled by quadrilateral shell elements (QUAD4) with composite laminate properties. The offset command was used to model the separate surfaces representing the beam web and rings. For linear buckling analysis accomplished with solution SOL 105 in Nastran, the C-section beam was loaded with a 20 *kN* vertical force at its free end through the shear centre. Buckling load and post-buckling load-deflection response was obtained by using the SOL 106 for nonlinear static solution.

Since the flange buckling stability is more critical than the web panel and stress concentration at web cutout, effort has been made to reinforce the flange and improve the overall buckling stability of the C-section beams. In the post-buckling analysis, the usual laminate failure criterion is used to assess the ply failure of C-section beams. In the current case, the Tsai-Wu criterion expressed in terms of failure index (*FI*) shown below is used [23].

$$f_1\sigma_1 + f_2\sigma_2 + f_{11}\sigma_1^2 + f_{22}\sigma_2^2 + f_{66}\sigma_6^2 + 2f_{12}\sigma_1\sigma_2 < 1 \qquad (1)$$

where $f_1 = 1/F_{1t} - 1/F_{1c}$, $f_{11} = 1/\left(F_{1t}F_{1c}\right)$, $f_2 = 1/F_{2t} - 1/F_{2c}$, $f_{22} = 1/\left(F_{2t}F_{2c}\right)$, $f_{66} = 1/F_6^2$, $f_{12} = G/\sqrt{F_{1t}F_{1c}F_{2t}F_{2c}}$, and F_{1t}, F_{1c}, F_{2t}, F_{2c} represents the lamina tensile and compressive strength in longitudinal direction-1 and in transverse direction-2 respectively; F_6 is the shear strength and a factor G = -0.5. In MSC Patran/Nastran, open the input window of Anisotropic Properties, select "Tsai-Wu" in the item of "Composite Failure Theory". Then the setting of failure criterion is completed.

2.3. Experiment setup

The C-section beams were manufactured and cured in an autoclave at 6 bar and 180ºC for a total cure time of 7 hours. The cutouts in the beam were made using a water jet cutting machine. As shown in Fig. 3, the C-section beam is clamped at one end and a downward vertical load was applied at the other free end through the section shear centre. A steel element bonded to the free end was used to distribute the load within the cross section.

3. Results and Discussion

3.1. Experimental and numerical strain results

With the test setup shown in Fig. 3, the C-section lower flange subject to a compressive stress was more critical than the web panel in terms of buckling instability. In order to detect the buckling behaviour of the C-section, strain gauges were placed at the predicted buckling location on the upper and lower surfaces of the lower flanges. Experiment of a C-section beam with an unreinforced circular cutout on the web was performed with strain measurement for validation purpose.

In the first experiment, a static shear force was applied to 20 kN with the results shown in Fig. 4(a). For this case, both linear and nonlinear solutions in FE analysis using Nastran SOL 101 and SOL 106 code were carried out for comparison. In this pre-buckling test, noticeable bending of the lower flange was observed. This is also shown in the different strain result of the upper and lower surfaces of the lower flange. It indicates the necessity of geometrical nonlinear analysis in the modelling of even the pre-buckling case. The results also indicate that linear analysis (dashed lines in Fig. 4a) could not capture the difference and not suitable for buckling analysis.

In the second experiment, the load applied to the C-section beam was increased to 25 kN beyond buckling. The comparison of measured and nonlinear FE strain results are shown in Fig. 4(b). From the results, critical buckling load can be determined when the strain on the top surface starts to decrease and the strain curvature on bottom surface starts to increase. The measured critical buckling load is about 22 kN, while the FE result shows about 20 kN. The difference is likely caused by setting the clamp condition along the bolt line in the FE model and ignoring the clamping pad especially at the lower flange root in real case. It is also observed that the experimental results in the second test are slightly different from the first one due to local failure around the bolts at the clamping end. After local reinforcement, the second test loading was increased but terminated at 25 kN.

3.2. Buckling and cutout effect analysis

After the FE model validation, the MSC Nastran linear solution sequences SOL 105 was applied to predict the buckling load. Numerical analysis was performed to assess the effect of different cutout shape and reinforcements on the buckling behaviour of the C-section beam. As shown in Fig. 5, the buckling load factor (BLF), which is defined as the ratio of the critical buckling load to the applied load, was 1.28 for the C-section without cutout when a load of 20 kN was applied. For the C-section with a diamond cutout, the BLF was reduced to 1.27. For the C-section with a circular cutout, the BLF has slightly more reduction to 1.266. This gives a buckling load of 25.3 kN, which is greater than the earlier nonlinear prediction shown in Fig.4. It shows again that the linear analysis is not accurate, but the prediction can be used as a relative figure to assess the cutout and reinforcement effect. Different cutout reinforcements were then added onto the C-section web. Numerical results show that the reinforcement rings made of steel, composite fibre tows and laminate have little effect on the BLF or even slightly higher BLF than the baseline C-section without cutout. The C-section with circular cutout and fibre tow reinforcement has the highest BLF of 1.308 (increased by 2.27%).

The analysis also shows that the cutout reinforcement can increase the web panel buckling stability significantly. However the web buckling of the C-section with a circular cutout is in much higher mode and the BLF is 3.92. It is therefore not the concern of the current investigation.

In order to increase the flange critical buckling load, three different flange reinforcements introduced in 2.1 were assessed for the C-section beam with circular cutout. The BLF for the beam with and without flange reinforcement are summarized in Table 2 and shown in Fig. 6. It can be observed that all the three reinforcements make a significant increase to the buckling stability of the beam. Since buckling occurred at the lower flange close to the clamp end, a relatively larger cross-section stiffener placed in this region (Re1) is more effective than a longer stiffener of a smaller cross-section (Re2). Identifying and reinforcing the critical region is a considerably effective way to improve the design of this type of C-section beam.

3.3. Nonlinear buckling and post-buckling response

For accurate post-buckling prediction, nonlinear analysis was performed on the C-section beams with and without cutout. Figure 7 shows the deflection of the beam under a shear load of 28 kN as an example. The deflection is measured from the original position in Y-direction. The results also show that the maximum bending moment and stress occurs at the interaction of web and flange where the first-ply failure actually occurs. The shear load was applied until the failure of the laminate. Figure 8 shows the load-deflection response of the beam. From Fig. 8a, the C-section beam without cutout reached first-ply-failure at a load of 29.49 *kN*. The diamond cutout leads to a decrease of failure load by 3.46% to 28.47 *kN*, while the circular cutout only by 0.61% to 29.31 *kN*. The maximum deflection of the beam with circular cutout increased from 10.52 mm to 11.32 mm, while the beam with diamond cutout had a slightly reduced deflection to 10.08 mm.

In order to increase the post-buckling failure load, the three L-shape stiffeners Re1 to Re3 were added to the C-section beam with a circular cutout and the analysis results are shown in Fig. 8b. It's interesting to note that the maximum deflection of the beam with Re1 or Re2 stiffeners is greater than the beam without reinforcement before buckling. The Re1 reinforcement shows a better performance with a first-ply-failure load of 33.18 *kN* than the Re2 with the load of 32.26 *kN*. The Re3 reinforcement shows the best buckling and post-buckling performance with the first-ply-failure load increased by 20.88% from 29.31 *kN* to 35.43 *kN*. However, serious stress concentration will be caused at the point connecting the reinforcement. If the flange reinforcement Re3 is applied for actual C-section beam, additional reinforcement has to be used to reduce the stress concentration at the flange near the end of Re3.

4. Conclusions

Buckling analysis of a C-section beam with an unreinforced circular cutout was performed numerically and experimentally. The results indicate that nonlinear method is necessary to predict the buckling load, while liner method is not suitable for buckling analysis. Based on the validation of FE model and buckling analysis of a C-section beam subjected to a shear load by experiment, the effects of cutout, edge reinforcement and flange reinforcements on the bucking load factor, post-buckling response, and first-ply-failure load were investigated.

Both diamond and circular cutouts on the C-section web cause a slight decrease in the critical buckling load by no more than 1.02%. Cutout reinforcements can increase the buckling stability and make the buckling load higher than the beam without cutout. Three reinforcements of steel, laminate, and fibre tow rings were considered. The C-section beam with circular cutout and tow reinforcement shows the highest buckling load factor.

Two horizontal L-shape stiffeners with the same material, layup, and weight bonded to the lower flange aligned with the cutout position were investigated. The numerical results show that the relatively larger cross-section stiffener placed in the buckling region is more effective than the longer stiffener of a smaller cross-section. So it is necessary to identify the buckling critical region for the reinforcement of the C-section. The same stiffener in vertical direction offers the most effective reinforcement to increase the first-ply-failure load by 20.88%.

References

[1] Ukadgaonker VG, Rao DKN. A General Solution for Stresses around Holes in Symmetric Laminates under Inplane Loading. Composite Structures 2000; 49(3): 339-354.

[2] Rezaeepazhand J, Jafari M. Stress Analysis of Perforated Composite Plates. Composite Structures 2005; 71(3-4): 463-468.

[3] Whitworth HA, Mahase H. Failure of Orthotropic Plates Containing a Circular Opening. Composite Structures 1999; 46(1): 53-57.0020

[4] Arjyal BP, Katerelos DG, Galiotis C, Filiou C. Measurement and Modeling of Stress Concentration around a Circular Notch. Experimental Mechanics 2000; 40(3): 248-255.

[5] Falzon BG, Steven GP, Xie YM. Shape Optimization of Interior Cutouts in Composite Panels. Structural and Multidisciplinary Optimization 1996; 11(1-2): 43-49.

[6] Guo S. Stress Concentration and Buckling Behaviour of Shear Loaded Composite Panels with Reinforced Cutouts. Composite Structures 2007; 80(1): 1-9.

[7] Kumar D, Singh S.B. Stability and failure of composite laminates with various shaped cutouts under combined in-plane loads. Composites Part B 2012; 43: 142-149.

[8] Kumar D, Singh S.B. Effects of flexural boundary conditions on failure and stability of composite laminate with cutouts under combined in-plane loads. Composites Part B 2013; 55: 433-439.

[9] Guo S, Morishima R, Zhang X, Mills A. Cutout Shaped and Reinforcement Design for Composite C-Section Beams under Shear Load. Composite Structures 2009; 88(2): 179-187.

[10] Nemeth MP. Buckling and Postbuckling Behaviour of Laminated Composite Plates with a Cutout. NASA Technical Paper 3587, 1996.

[11] Bailey R, Wood J. Stability Characteristics of Composite Panels with Various Cutout Geometries. Composite Structures 1996; 35(1): 21-31.

[12] Eiblmeier J, Loughlan J. The Influence of Reinforcement Ring Width on the Buckling Response of Carbon Fibre Composite Panels with Circular Cutouts. Composite Structures 1997; 38(1-4): 609-622.

[13] Eiblmeier J, Loughlan J. The buckling response of carbon fibre composite panels with reinforced cutouts. Composite Structures 1995; 32(1-4): 97-113.

[14] Eryigit E, Zor M, Arman Y. Hole effects on lateral buckling of laminated cantilever beams. Composites Part B 2009; 40: 174-179.

[15] Pasinli A. Shape and position effects of double holes on lateral buckling of cantilever composite beams. Composites Part B 2013; 55: 433-439.

[16] Dung DV, Hoa LK. Research on nonlinear torsional buckling and post-buckling of eccentrically stiffened functionally graded thin circular cylindrical shells. Composites Part B 2013; 51: 300-309.

[17] Shi S, Sun Z, Ren M, Chen H, Hu X. Buckling response of advanced grid stiffened carbon-fiber composite cylindrical shells with reinforced cutouts. Composites Part B 2013; 44: 26-33.

[18] Jegley DC, Tatting BF, Adoptech J, Gürdal Z. Optimization of Elastically Tailored Tow-Placed Plates with Holes. 44th AIAA/ASME/ASCE/AHS/ASC Structures, Structural Dynamics, and Materials Conference, Norfolk, Virginia, 2003.

[19] Lopes CS, Gürdal Z. Progressive Failure Analysis of Tow-Placed, Variable-Stiffness Composite Panels. 48th AIAA/ASME/ASCE/AHS/ASC Structures, Structural Dynamics, 2007.

[20] Razzaq Z, Prabhakaran R, Sirjani MM. Load and Resistance Factor Design (LRFD) Approach for Reinforced-Plastic Channel Beam Buckling. Composites Part B: Engineering 1996; 27(3-4): 361-369.

[21] Lee J, Kim, SE. Lateral Buckling Analysis of Thin-Walled Laminated C-Section Beams. Composite Structures 2002; 56(4): 391-399.

[22] Shan L, Qiao P. Flexural-Torsional Buckling of Fiber-Reinforced Plastic Composite Open Channel Beams. Composite Structures 2005; 68(2): 211-224.

[23] Tsai SW, Wu EM. A general theory of strength for anisotropic materials. Journal of Composite Material 1971; 5: 58-80.

Table 1: Mechanical properties of Hexply M21/T800S prepreg*

E_1 (GPa)	E_2 (GPa)	G_{12} (GPa)	ν_{12}	X_t (MPa)	X_c (MPa)	Y_t (MPa)	Y_c (MPa)	S (MPa)	ρ (kg/m^3)
172	10	5	0.3	3939	1669	50	250	79	1580

* Data source: http://www.hexcel.com/products/matrix%20products/prepregs, accessed 4 Sept 2007.

Table 2: Buckling load factor with cutout and flange reinforcement (Re)

	No Re	Re1	Re2	Re3
Without cutout	1.279	1.705	1.633	1.594
Diamond cutout	1.269	1.669	1.611	1.525
Circular cutout	1.266	1.633	1.622	1.509

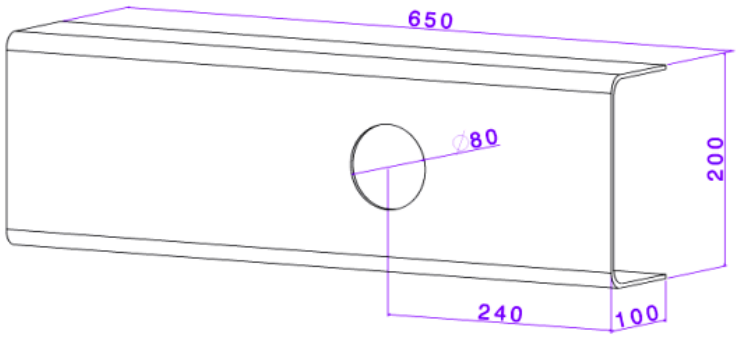

a.

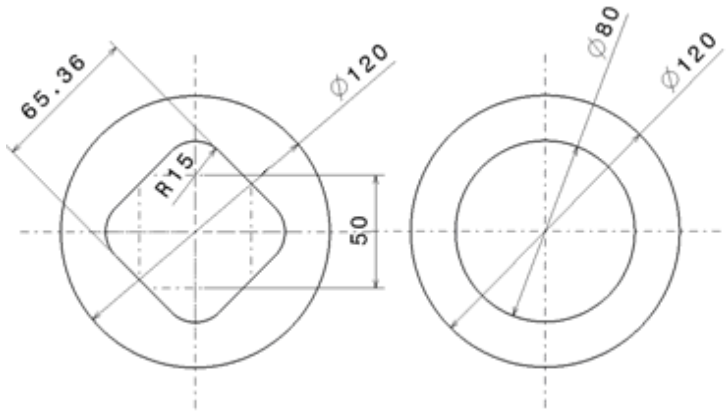

b.

Fig. 1. (a) A C-section beam with circular cutout; (b) Dimensions of the diamond and circular cutouts and reinforcement rings (in mm).

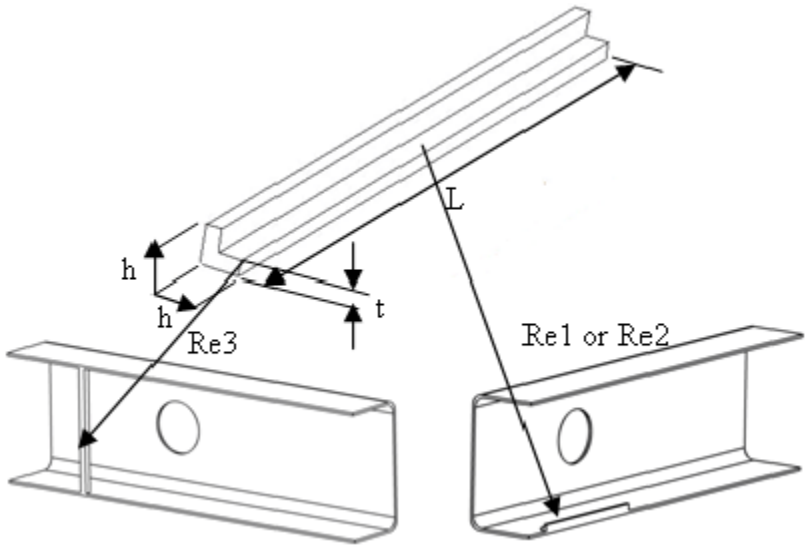

Fig. 2. Positions of L-shaped reinforcement flange and dimensions, Re1: h = 10mm, t = 4 mm, L = 200 mm; Re2: h = 5mm, t = 4 mm, L = 400 mm; Re3: h = 10mm, t = 4 mm, L = 200 mm.

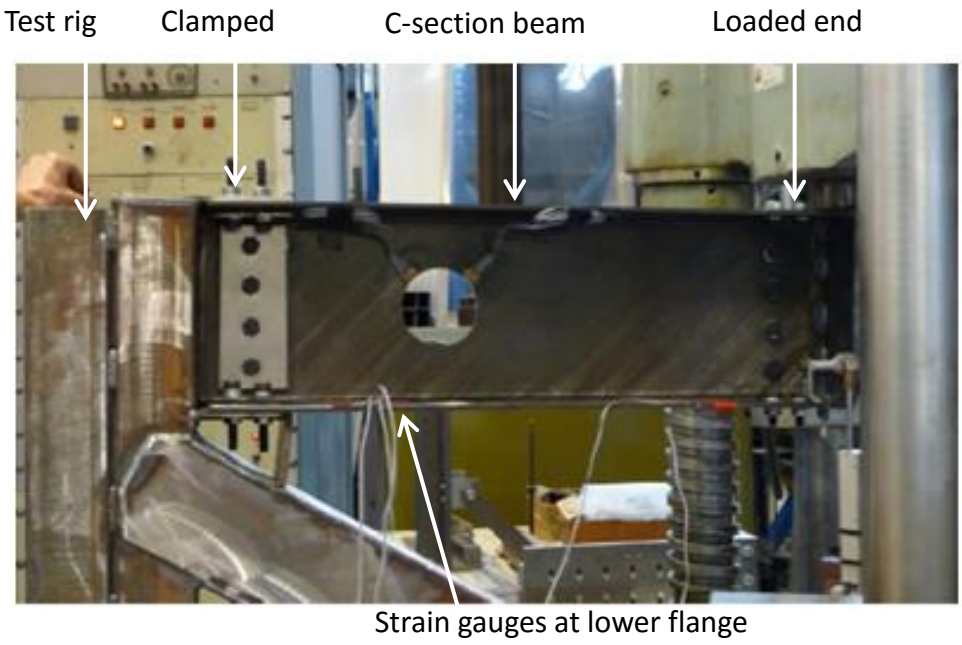

Fig. 3. C-section beam mounted on the testing rig

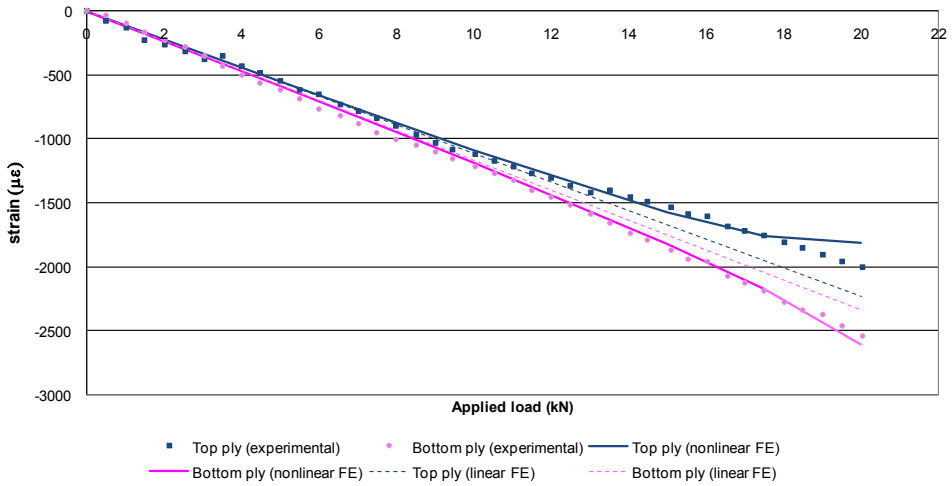

(a)

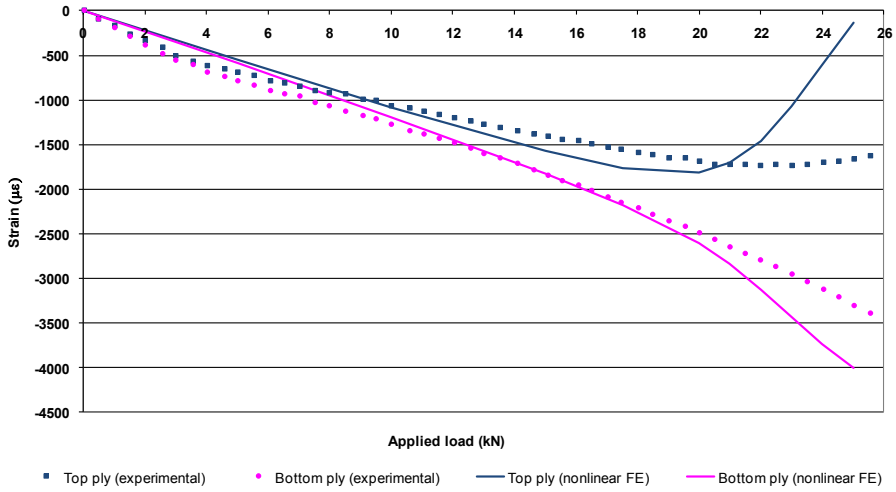

(b)

Fig. 4. Experimental and FE strain results at lower flange: (a) the first test; (b) the second test

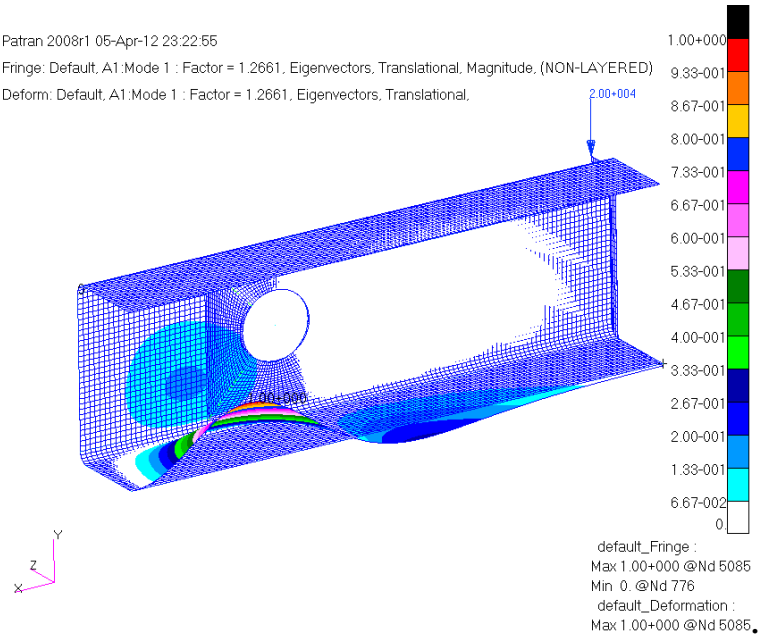

Fig. 5. The first buckling mode under a load of 20 kN

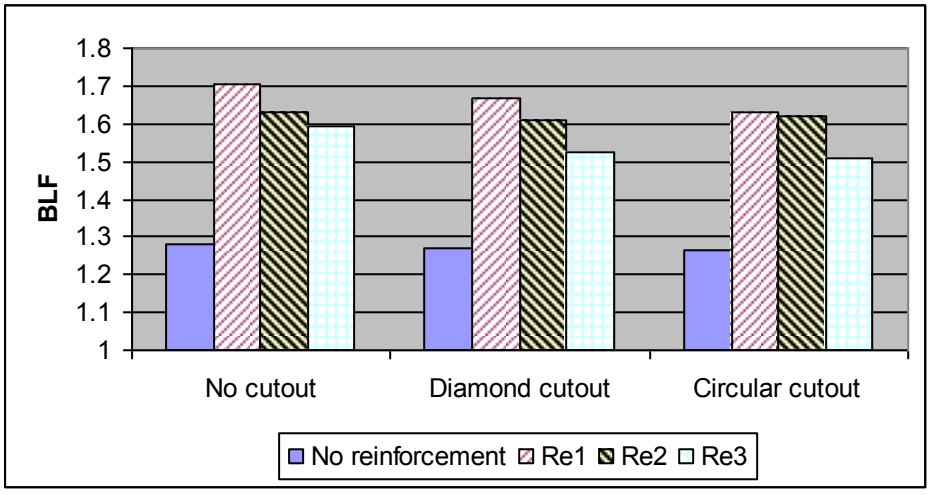

Fig. 6. Effect of cutout and edge reinforcement on Lower flange buckling.

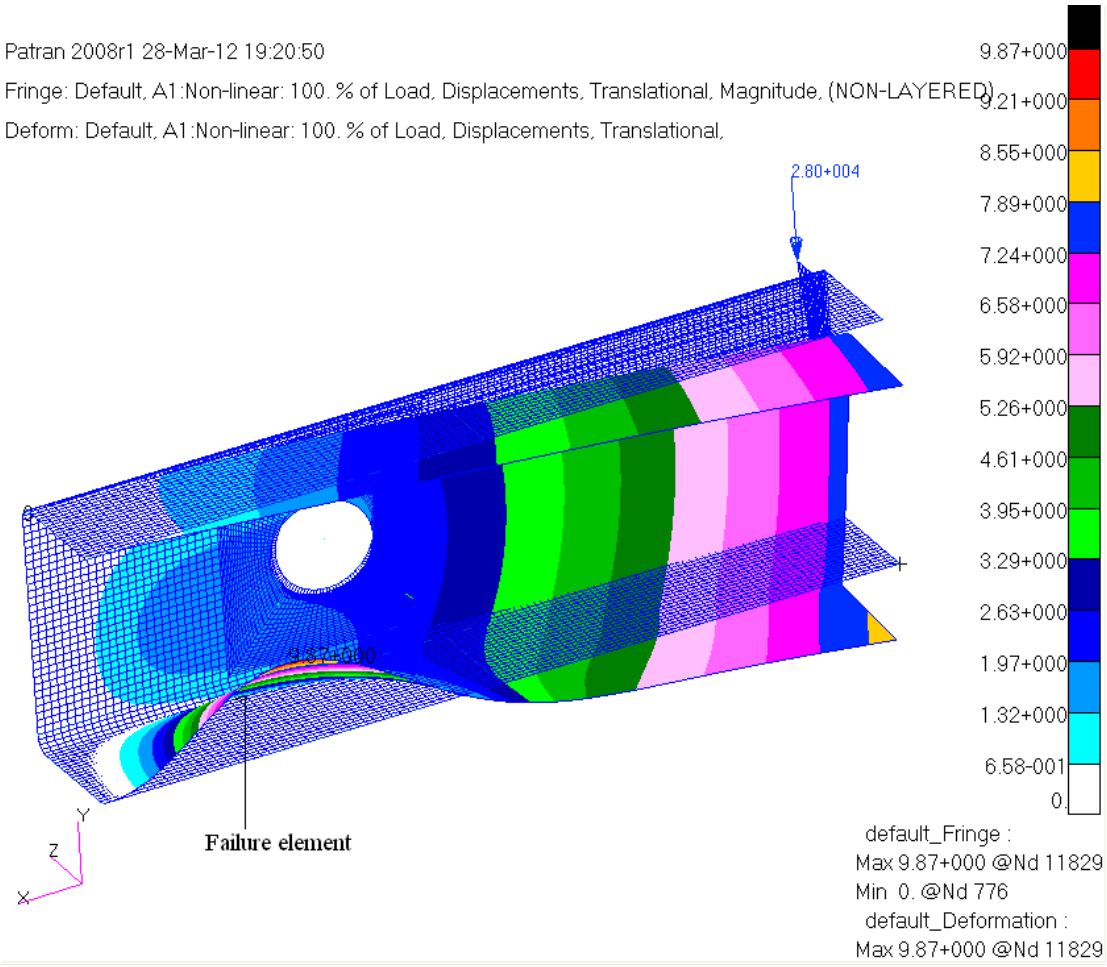

Fig. 7. Nonlinear deflection of the C-section beam under shear load 28 kN

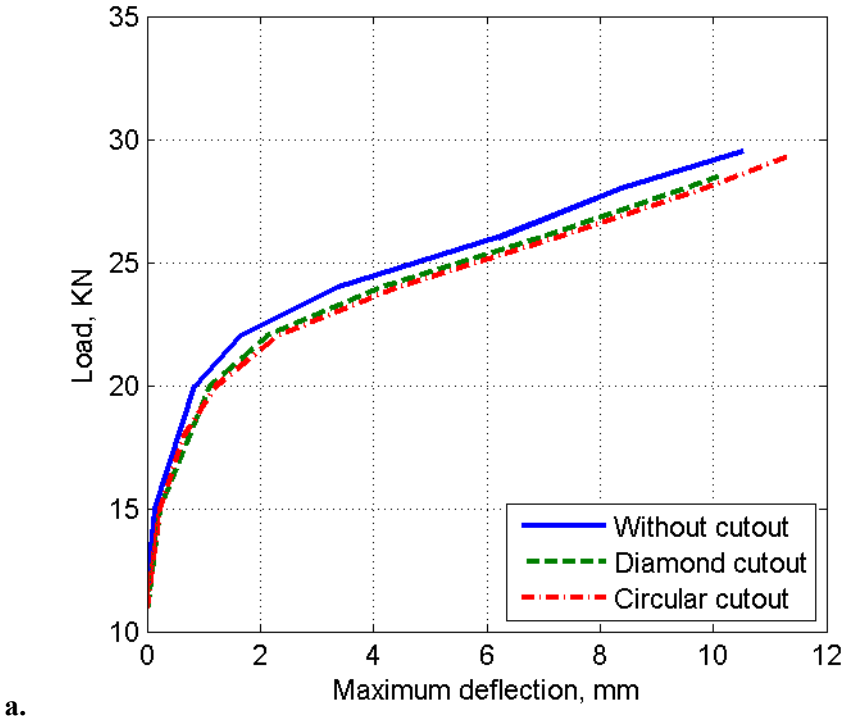

a.

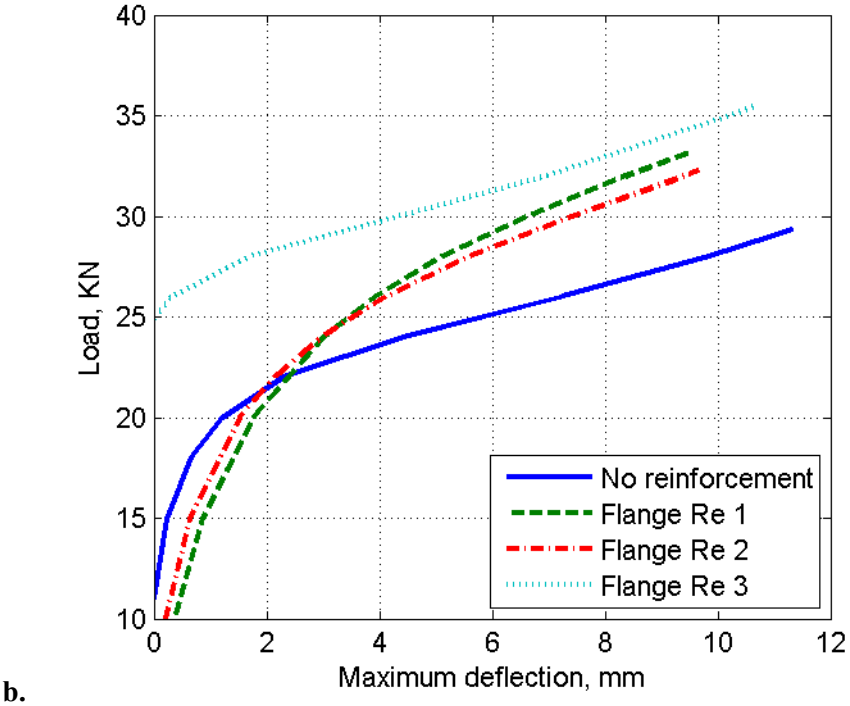

b.

Fig. 8. Load-deflection responses of the C-section beam with: (a) different cutouts; (b) different flange reinforcement